Journal of Solid State Chemistry 184 (2011) 2707–2712

Contents lists available at SciVerse ScienceDirect

Journal of Solid State Chemistry

journal homepage: www.elsevier.com/locate/jssc

Ternary system Er–Ni–In at $T=870$ K

M. Dzevenko [a,*], Yu. Tyvanchuk [a], L. Bratash [a], V. Zaremba [a], L. Havela [b], Ya. Kalychak [a]

[a] Department of Analytical Chemistry, Ivan Franko National University of Lviv , Kyryla and Mefodiya Str. 6, UA-79005 Lviv, Ukraine
[b] Department of Condensed Matter Physics, Charles University, Prague, Ke Karlovu 5, 121 16 Praha 2, Czech Republic

ARTICLE INFO

Article history:
Received 29 April 2011
Received in revised form
3 August 2011
Accepted 9 August 2011
Available online 16 August 2011

Keywords:
Ternary system Er–Ni–In
Isothermal section
Crystal structure
Solid solution
Physical properties

ABSTRACT

Isothermal section of the Er–Ni–In system at $T=870$ K was constructed by means of X-ray powder diffraction and EDX-analyses. Nine ternary compounds, namely $ErNi_9In_2$ (YNi_9In_2-type), $Er_{1-1.22}Ni_4In_{1-0.78}$ ($MgCu_4Sn$-type), $Er_{10}Ni_{9.07}In_{20}$ ($Ho_{10}Ni_9In_{20}$-type), $ErNi_{1-0.60}In_{1-1.40}$ (ZrNiAl-type), Er_2Ni_2In (Mn_2AlB_2-type), $Er_2Ni_{1.78}In$ (Mo_2FeB_2-type), $Er_5Ni_2In_4$ ($Lu_5Ni_2In_4$-type), Er_5Ni_2In (Mo_5SiB_2-type), and $Er_{13.53}Ni_{3.14}In_{3.33}$ ($Lu_{14}Co_2In_3$-type), exist in the Er–Ni–In system at this temperature. The substitution of Ni for In was observed for $ErNi_{1-0.60}In_{1-1.40}$ and In for Er in the case of related compounds $ErNi_2$ and $ErNi_4In$. Er can enter NiIn (CoSn-type) leading to including-substitution type of compound $Er_{0-0.12}NiIn_{1-0.89}$. Basic magnetic properties of the $Er_{0.04}NiIn_{0.97}$, $ErNi_2$, $Er_{0.9}Ni_2In_{0.1}$, and $ErNi_4In$ phases were inspected. Electrical-resistivity studies were performed on the ErNiIn, $ErNi_{0.9}In_{1.1}$, and $ErNi_4In$ phases.

1. Introduction

A general effort to extend our knowledge of materials with various characteristics led us to exploration of metallic systems including ternary rare earth systems with *d*-metals and *p*-elements, which exhibit a large richness of phases [1]. This is true also for the *R*–Ni–In systems, where various crystals structures of ternary compounds have been determined. The isothermal sections of the phase diagram Ce–Ni–In have been constructed [2] and crystal structures of about 130 ternary indides have been identified in this and related systems [3,4].

The subject of the present work is the investigation of components interaction in the Er–Ni–In ternary system. A complete isothermal section in the full concentration range at $T=870$ K has been constructed, with the focus on phases existing over a certain homogeneity regions. Selected compounds were briefly characterized as to their magnetic properties. Some preliminary results were presented in Ref. [5].

The temperature of investigation was chosen to correspond a state, which can be easily obtained by annealing. In general, the annealing temperature must be as high as possible for the fast achieving a homogenization; on the other hand, the samples must be in solid state. The annealing temperatures for majority of investigated ternary systems *R*–*d*-metals–*X* (R–rare earth, X–Si, Ge, Al, Ga, and In) are in the 770–1070 K range. For the case of indides, the annealing temperature $T=870$ K is quite favourable and has been used in many cases [1].

The binary systems Er–Ni [6], Ni–In [7–9], and Er–In [10], which are around the investigated ternary system, were studied in quite some detail. The phase diagrams of these systems have been constructed and crystal structures of binary compounds determined. Concerning the phase diagram of the Ni–In binary system, the small differences in homogeneity regions and melting temperatures of binary compounds exist in the literature. The Er–Ni, Ni–In, and Er–In binary systems are characterized by complicated interaction of components. The rather large number of binary compounds form in all these systems: 11 binary compounds exist in the Er–Ni system, 8—in the Ni–In system, and 5—in the Er–In system. In addition, a limited solubility of In in Er and Ni exist in the Er–In and Ni–In binary systems, and only Er_5In_3, $Ni_{13}In_9$, phases ζ, and δ form homogeneity regions.

2. Experimental

Starting materials for the preparation of the alloys were ingots of the erbium and nickel, and indium tear drops, all with nominal purities better than 99.9%. 73 ternary and two binary samples (of a typical mass of 1–2 g) were synthesized by melting the pure elements in an arc-furnace on a water-cooled Cu-plate under an argon atmosphere (sponge Ti was used as a getter). The buttons were turned over and remelted two times to ensure homogeneity. The weight losses were smaller than 1% in all cases. The alloys were subsequently sealed in evacuated silica tubes and annealed at $T=870$ K for 720 h and quenched in cold water without

* Corresponding author.
E-mail address: mashadzev@gmail.com (M. Dzevenko).

0022-4596/$ - see front matter © 2011 Elsevier Inc. All rights reserved.
doi:10.1016/j.jssc.2011.08.006

breaking the tubes. Chemical and phase compositions of samples are shown in Fig. 1.

Investigation of the isothermal sections of Er–Ni–In ternary systems was carried out by X-ray powder diffraction method. The X-ray phase analysis was performed using film data (Debye–Scherrer technique, RKD-57.3 camera, Cr–*K*-radiation) and powder diffractometers (DRON-2.0, Fe–*K*α-radiation, Ge as an internal standard; Seifert XRD7, Cu–*K*α-radiation).

The indexing of the obtained diffraction data of the ternary alloys was performed by comparison with calculated data (the program Powder Cell [11]). The lattice parameters of some phases were calculated using the program LATCON [12]. In selected cases the composition of some samples was analyzed in a scanning electron microscope (LEICA 420i) by means of electron microprobe analysis using ErF_3, Ni, and InAs as standards.

Magnetic measurements were performed in the temperature range 2–300 K in magnetic field up to 6 T by means of extraction magnetometer (Quantum Design PPMS) in the form of powder sample with randomly oriented grains fixed by a glue. The electrical resistivity was measured by four-probe method in the temperature range 80–380 K for $ErNi_{0.9}In_{1.1}$ and ErNiIn phases and 4–300 K for the $ErNi_4In$ compound.

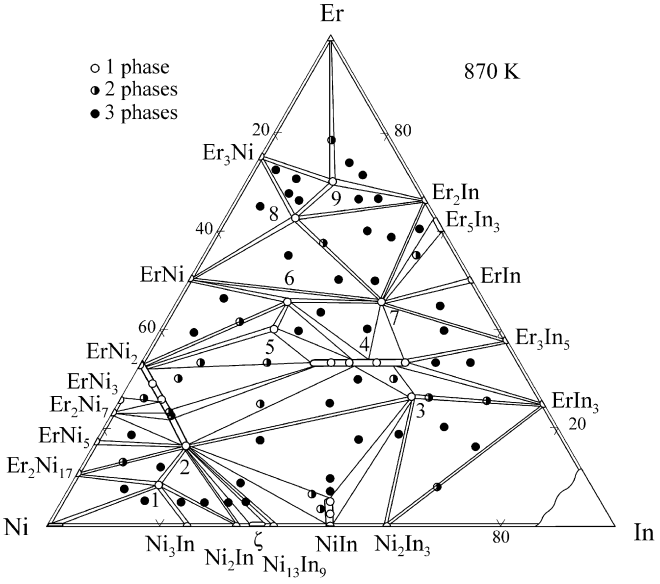

Fig. 1. Chemical and phase composition of samples and isothermal section of the Er–Ni–In system at $T=870$ K.

3. Results

3.1. The phase analysis of Er–NI–in ternary system

The isothermal section of Er–Ni–In ternary system at $T=870$ K is shown in Fig. 1. It was confirmed that at 870 K the following binary compounds exist: Er_2In (Ni_2In-type), Er_5In_3 (Mn_5Si_3-type), ErIn (CsCl-type), Er_3In_5 (Pu_3Pd_5-type), $ErIn_3$ ($AuCu_3$-type); Er_3Ni (Fe_3C-type), ErNi (FeB-type), $ErNi_2$ ($MgCu_2$-type), $ErNi_3$ ($NbBe_3$-type), Er_2Ni_7 (Gd_2Co_7-type), $ErNi_5$ ($CaCu_5$-type), Er_2Ni_{17} (Th_2Ni_{17}-type); Ni_3In (Ni_3Sn-type), Ni_2In (Ni_2In-type), phase ζ (Ni_xIn_{1-x}, NiAs-type), $Ni_{13}In_9$ ($Ni_{13}Ga_9$-type), NiIn (CoSn-type), phase δ (Ni_xIn_{1-x}, CsCl-type), and Ni_2In_3 (Ni_2Al_3-type). Almost none of the binary compounds dissolve the third component. The exception is the existence of solid solutions based on NiIn and $ErNi_2$ binary compounds.

The phase equilibrium of Er–Ni–In system at 870 K is characterized by the formation of nine ternary compounds with crystallographic parameters given in Table 1. Rodewald et al. [36] reported on existence of $Er_{2.30}Ni_{1.84}In_{0.70}$. The authors succeeded to extract a single crystal of it from arc-melted sample and determined that the $Er_{2.30}Ni_{1.84}In_{0.70}$ compound crystallizes with a new superstructure upon the Mo_2FeB_2 type. We did not find this compound in samples annealed at 870 K. Instead Er_2Ni_2In (Mn_2AlB_2-type) [34] and $Er_2Ni_{1.78}In$ (Mo_2FeB_2-type) [35] were indicated in the present study. The reason of the discrepancy may be in the fact that $Er_{2.30}Ni_{1.84}In_{0.70}$ may be thermodynamically stable only at higher temperatures.

3.2. $ErNi_{1-0.60}In_{1-1.40}$ ternary compound

The ternary compound ErNiIn crystallizes in the ZrNiAl structure type. The homogeneity region was determined for this compound across the section 33.3 at% Er [13]. Variations of lattice parameters of some samples revealed that the homogeneity region extends from 33.3 to 46.6 at% In (Fig. 2a) and the composition of compound is described by the formula $ErNi_{1-0.60}In_{1-1.40}$. The volume and the lattice parameter *a* increase (*c* decreases) in the homogeneity range of $ErNi_{1-0.60}In_{1-1.40}$ due to the substitution of smaller atoms of Ni by larger atoms of In.

Gondek et al. [14] and Tyvanchuk et al. [15] reported on magnetic properties of this compound. The magnetic behaviour changes from ferromagnetic for equiatomic composition ($T_C=9$ K) to antiferromagnetic (with similar ordering temperatures) for non-stoichiometric one with increase in indium content. Two samples of ErNiIn and $ErNi_{0.9}In_{1.1}$ were chosen for the electrical resistivity study (Fig. 3). The values of resistivity at $T=80$ K are

Table 1
Crystallographic characteristics of ternary compounds in the Er–Ni–In system.

No.	Compound	Structure type	Space group	Lattice parameters (nm)			Refs.
				a	*b*	*c*	
1	$ErNi_9In_2$	YNi_9In_2	*P*4/*mbm*	0.8190	–	0.4801	[28]
2	$ErNi_4In$	$MgCu_4Sn$	$F\bar{4}3m$	0.6996	–	–	[29]
	$Er_{1-1.22}Ni_4In_{1-0.78}$			0.6993–0.7017	–	–	[17]
3	$Er_{10}Ni_{9.07}In_{20}$	$Ho_{10}Ni_9In_{20}$	*P*4/*nmm*	1.3250	–	0.9070	[30]
				1.3230	–	0.9052	[31]
				1.3254	–	0.9064	[32]
4	ErNiIn	ZrNiAl	$P\bar{6}2m$	0.7441	–	0.3723	[33]
	$ErNi_{1-0.60}In_{1-1.40}$			0.7412–0.7656	–	0.3739–0.3693	[13–15]
5	Er_2Ni_2In	Mn_2AlB_2	*Cmmm*	0.3893	1.4110	0.3639	[34]
6	$Er_2Ni_{1.78}In$	Mo_2FeB_2	*P*4/*mbm*	0.7310	–	0.3654	[35]
	$Er_{2.30}Ni_{1.84}In_{0.70}$	$Er_{2.3}Ni_{1.84}In_{0.7}$	*P*4/*m*	0.7386	–	0.3614	[36]
7	$Er_5Ni_2In_4$	$Lu_5Ni_2In_4$	*Pbam*	1.7722	0.7866	0.3558	[37]
8	Er_5Ni_2In	Mo_5SiB_2	*I*4/*mcm*	0.7546	–	1.3169	[38]
9	$Er_{13.53}Ni_{3.14}In_{3.33}$	$Lu_{14}Co_2In_3$	$P4_2/nmc$	0.9442	–	2.2691	[39]

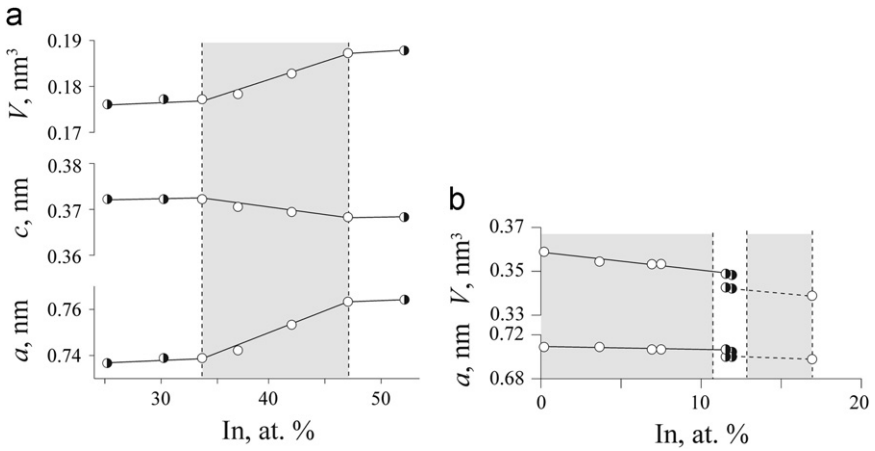

Fig. 2. Dependence of the lattice parameters and the unit cell volume V of $ErNi_{1-0.60}In_{1.00-1.40}$ (a), and $Er_{1-0.68}Ni_2In_{0-0.32}$ and $Er_{1-1.22}Ni_4In_{1-0.78}$ compounds (b) vs. the concentration of In.

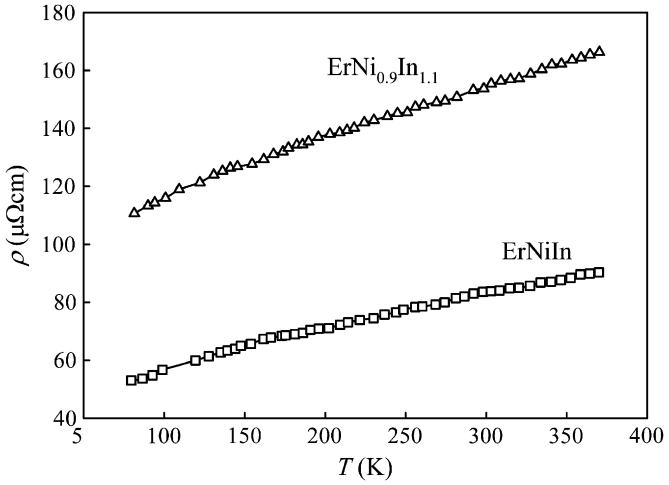

Fig. 3. Temperature dependence of electrical resistivity of ErNiIn and $ErNi_{0.9}In_{1.1}$. The absolute accuracy of resistivity values, given by uncertainty of the geometrical factor, is typically better than 10%.

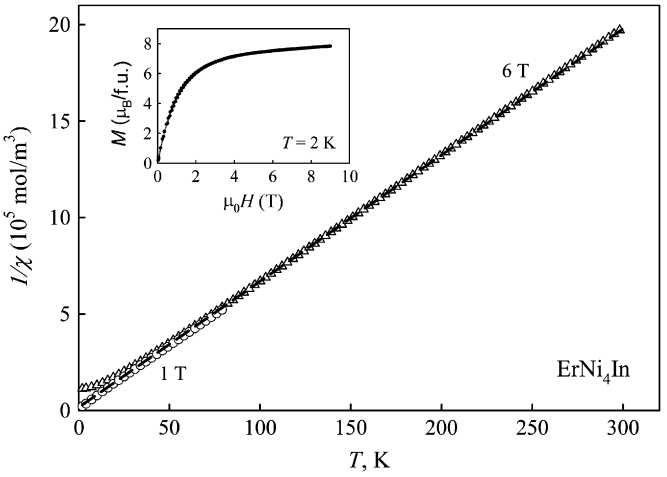

Fig. 4. Temperature dependence of inverse magnetic susceptibility of $ErNi_4In$ in various magnetic fields. The data for $\mu_0H=1$ T (circles) follow the dashed line, representing the fit to the CW law. The data in $\mu_0H=6$ T (triangles) show a saturation at the low-T limit. Its reason is seen in the inset, capturing the field dependence of magnetization of $ErNi_4In$, measured $T=2$ K.

0.53 and 1.11 μΩm for ErNiIn and $ErNi_{0.9}In_{1.1}$, respectively, and they increase almost linearly to $T=300$ K reaching 0.84 and 1.55 μΩm, respectively. The linear increase at high temperatures is typical for electron–phonon scattering [16]. The higher resistivity values for $ErNi_{0.9}In_{1.1}$ can be explained by higher atomic disorder, leading to a random potential causing additional temperature independent scattering of conduction electrons [16].

3.3. $Er_{1-0.68}Ni_2In_{0-0.32}$ and $Er_{1.22-1}Ni_4In_{0.78-1}$ phases

The ternary compound $ErNi_4In$ ($MgCu_4Sn$-type structure, space group $F\bar{4}3m$) is closely related to the Laves phase $ErNi_2$ ($MgCu_2$-type structure, space group $Fd\bar{3}m$). The small difference in size of Er and In atoms and the relation between the structures allow an opposite solubility between these two compounds. Therefore a solid solution based on $ErNi_2$ and homogeneity region of $ErNi_4In$ ternary compound are along the section 66.7 at% Ni and the composition the phases may be described as $Er_{1-0.68}Ni_2In_{0-0.32}$ and $Er_{1.22-1}Ni_4In_{0.78-1}$ (Fig. 2b). In the phase with $MgCu_2$-structure type, the site of Mg atoms (Wyckoff position 8*b*) is occupied by a statistical mixture of Er and In atoms. In the case of ternary $Er_{1.22-1}Ni_4In_{0.78-1}$, the substitution of Er atoms by In atoms take place at the 4*c* site [17].

In addition, we measured the magnetic susceptibility of $ErNi_4In$, which can be compared with the data on $ErNi_2$ and $Er_{0.9}Ni_2In_{0.1}$ reported in Ref. [17]; results are displayed in Fig. 4. The temperature range applied captures the paramagnetic state with the susceptibility following the Curie–Weiss law. The paramagnetic Curie temperatures Θ_p for $ErNi_2$, $Er_{0.9}Ni_2In_{0.1}$, and $ErNi_4In$ phases are 32 K, 24 K, and −2.6 K, respectively. The effective magnetic moments per Er ion for all these compounds are close to the theoretical effective moment of Er^{3+} ions (9.58 μ_B) and are 9.1(1), 9.1(2) and 9.90(1) μ_B. The similar value for $ErNi_2$ (9.37 μ_B) was reported in Ref. [18]. The saturated magnetization approaches 8 μ_B/Er atom in this case, i.e. approaching the theoretical value 9.0 μ_B. The saturation in high fields (i.e. the non-linearity of the Brillouin function describing the response of magnetization of local moments to magnetic field) causes that the susceptibility in the low-temperature range becomes field dependent.

The temperature-dependent electrical resistivity of $ErNi_4In$ compound (Fig. 5) exhibits a common metallic behaviour without any sign of magnetic order. One can assume an antiferromagnetic ordering at still lower temperatures, as Θ_p is negative and small in absolute value.

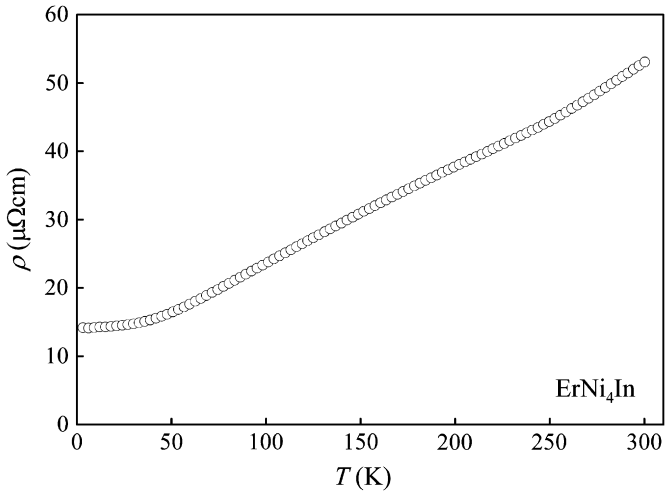

Fig. 5. Temperature dependence of electrical resistivity of $ErNi_4In$.

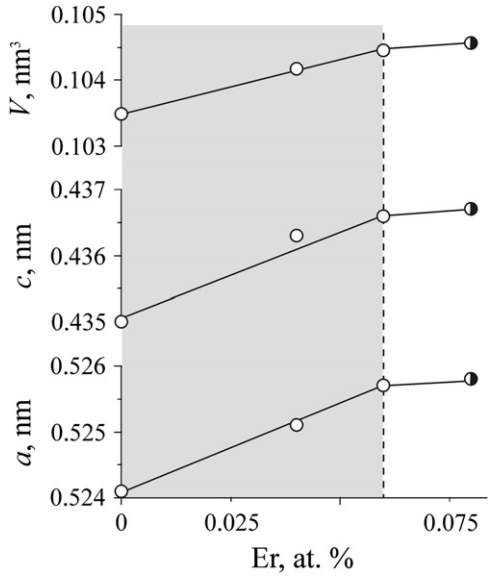

Fig. 6. Dependence of the lattice parameters and unit cell volume V vs. the content of Er in the solid solution based on NiIn.

3.4. $Er_{0-0.12}NiIn_{1-0.89}$ solid solution

The solid solution based on NiIn (CoSn-type structure, space group $P6/mmm$) exists in the Er–Ni–In system. The microprobe analysis results of $Er_{0.02}Ni_{0.49}In_{0.49}$, $Er_{0.04}Ni_{0.48}In_{0.48}$, and $Er_{0.06}Ni_{0.47}In_{0.47}$ samples show that they consist of a single-phase. The experimentally determined compositions of these samples were close to the compositions of ingots and can be described as $Er_{0.02}Ni_{0.49}In_{0.49}$, $Er_{0.05}Ni_{0.48}In_{0.47}$, and $Er_{0.07}Ni_{0.49}In_{0.44}$, respectively. In the samples with the composition $Er_{0.04}Ni_{0.50}In_{0.46}$ and $Er_{0.06}Ni_{0.50}In_{0.44}$ we observed the coexistence of the solid solutions based on NiIn and ternary compound $ErNi_4In$ (Fig. 1).

Therefore, the solid solution based on NiIn binary compounds ($a=0.5211$ nm, $c=0.4349$ nm) can be assumed as stable for 0–7 at% Er (Fig. 6). The increase in Er atoms content in the solid solution leads to the increase of lattice parameters (c/a remains approximately 0.83). According to Ref. [19], rather large interstitials exist in the CoSn-type structure, the centre of which are in the (0 0 1/2) position. Therefore, it was supposed that Er atoms enter this site. For more exact determination of Er atomic positions, the crystal structure of $Er_{0.02}Ni_{0.49}In_{0.49}$ and $Er_{0.04}Ni_{0.48}In_{0.48}$ samples were investigated using X-ray powder diffraction. The scattering density inside the unit cell of NiIn was calculated using the GFourier Program 04.04 for the both samples. It was determined that Er atoms really are located at (0 0 z) with $z\approx0.43$, which corresponds to the 2e Wyckoff site. The subsequent refinement of crystal structure was performed with the FullProf 3.40 program [20]. Crystal data and details of structure refinements are listed in Table 2. Fig. 7 shows the X-ray diffraction patterns of the respective samples [21].

In the NiIn binary compound, the Ni atom is coordinated by 10-vertices consisting of hexagon 4Ni+2In(1a) and a rectangle of 4In(2d). The six Ni atoms and nine In atoms (3In(2d)+6In(1a) form a 15-vertices polyhedron around In(2d). The coordination polyhedron around In(1a) is 20-vertices polyhedron consists of 6Ni+12In(2d)+2In(1a). The interatomic distances Ni–Ni and Ni–In(1a) are equal and shortest (0.2622 nm) in this structure. In case of the $Er_{0-0.12}NiIn_{1-0.89}$ phase, some changes in coordination sphere take place because of the Er atoms included. The coordination number of some Ni atoms becomes 11. Four Ni, one In(1a), four In(2d), and two Er atoms form the coordination sphere of Ni atoms. The coordination polyhedrons of In(2d) and In(1a) atoms are still 15- and 20-vertices polyhedrons, respectively, but one Er atom takes the place of one In(1a) in both coordination polyhedrons. The interatomic distances between Ni and In atoms change slightly. The equal distances Ni–Ni and Ni–In(1a) stay the shortest in the $Er_{0-0.12}NiIn_{1-0.89}$ phase (0.26256 nm). The distances between Ni, In, and Er atoms are given in Fig. 8.

The magnetic susceptibility of $Er_{0.04}NiIn_{0.97}$ phase obeys a modified Curie–Weiss law in the whole studied temperature range (Fig. 9), with the paramagnetic Curie temperature $\Theta_p=-11.6$ K and the temperature-independent term $\chi_0=-4.766\times10^{-9}$ m^3/mol. Such behaviour can be interpreted as presence of paramagnetic ions in a diamagnetic matrix. The effective magnetic moment 10.2 μ_B/Er is slightly enhanced with respect to the theoretical value for $4f^{11}$ (9.58 μ_B). Considering the error due to the low Er concentration, this difference is not significant. One should note that a spin polarization of the 5d and other electronic states, which can be often as high as 0.5 μ_B, can modify the 4f magnetic moments of rare-earth atoms in metals. On the other hand, the

Table 2
Results of structure refinements of $Er_{0.04}NiIn_{0.97}$ and $Er_{0.07}NiIn_{0.94}$ phases.

Sample composition	$Er_{0.02}Ni_{0.49}In_{0.49}$	$Er_{0.04}Ni_{0.48}In_{0.48}$
Calculated composition	$Er_{0.04}NiIn_{0.97}$	$Er_{0.07}NiIn_{0.94}$
Molar mass (g/mol)	176.76	178.33
Equipment	Seifert XRD7	Seifert XRD7
Wavelength	Cu$K\alpha$ (1.54178)	Cu$K\alpha$ (1.54178)
2Θ range for data collection	15.00°–130.00°	15.00°–130.00°
Step size in 2Θ (deg.)	0.02	0.02
Structure type	CoSn	CoSn
Space group	$P6/mmm$	$P6/mmm$
Lattice parameters (nm)	$a=0.52457(4)$	$a=0.52512(5)$
	$c=0.43578(4)$	$c=0.43637(4)$
Volume	$V=0.10385(2)$ nm^3	$V=0.10421(2)$ nm^3
Er at 2e (0 0 z)	$z=0.410(1)$	$z=0.3462(8)$
Occupation	0.065(6)	0.111(1)
B_{iso} (Å^2)	0.60(1)	1.05(1)
Ni at 3f (1/2 0 0)		
Occupation	1.00	1.00
B_{iso} (Å^2)	0.45(2)	0.59(2)
In1 at 2d (1/3 2/3 1/2)		
Occupation	1.00	1.00
B_{iso} (Å^2)	0.60(1)	1.05(1)
In2 at 1a (0 0 0)		
Occupation	0.91(1)	0.831(2)
B_{iso} (Å^2)	0.60(1)	1.05(1)
R_f (%)	4.25	6.32
R_{Bragg} (%)	5.82	7.28

saturated magnetization at $T=2$ K, which corresponds to only 5.0 μ_B/Er is considerably lower than the theoretical value 9.0 μ_B. The difference can be attributed e.g. to a strong magnetic anisotropy reducing the magnetization of randomly oriented grains.

4. Discussion

The interaction of indium with rare earths and 3*d*-metals has complex character due to different electron structure of interacting components. The large number of ternary compounds with various structure types exists in R–T–In systems. Almost all $R_xT_yIn_z$ ternary indides with large Ni content have a complicated multilayer structure with high coordination numbers of all types of atoms. Two-layer structure across the shortest period characterizes the compounds from the central part of the concentration triangle. Compounds with high rare-earth metals content as well as Ni-rich compounds have a complicated structure, but coordination numbers of the atoms are much smaller.

Nine ternary compounds were found to form in the investigated system Er–Ni–In at $T=870$ K. It is less than in the comparable system Ce–Ni–In (13 compounds), the isothermal section of which has been constructed [1,2], and other R–Ni–In systems, which have been partly explored testing the existence of isostructural compounds [1]. The common feature of the R–Ni–In systems is the formation of isostructural compounds RNi_9In_2 (YNi_9In_2-type structure), RNi_4In ($MgCu_4Sn$-type structure), RNiIn (ZrNiAl-type structure), and compounds with the Mo_2FeB_2-type structure. The fundamental difference between the Ce–Ni–In and Er–Ni–In systems is in the nature of solid solutions and homogeneity region of the compounds. In the first system, the compound with the Mo_2FeB_2-type structure is formed at the stoichiometric composition, but in the second case the same type structure is defective on Ni atoms ($Er_2Ni_{1.78}In$). The substitution of Ni for In atoms take place in homogeneity regions of $CeNi_{0.3-0.2}In_{1.7-1.8}$ ternary compounds with the AlB_2 type structure, while no compound with this type structure was found in

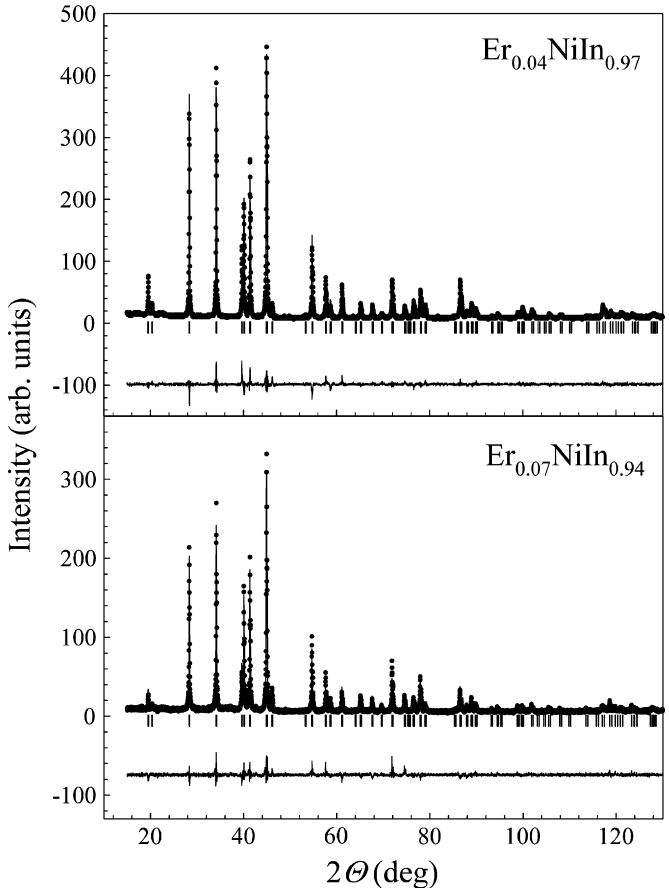

Fig. 7. Observed (◆) calculated (—) and difference X-ray diffraction patterns of the $Er_{0.04}NiIn_{0.97}$ and $Er_{0.07}NiIn_{0.94}$ (Seifert XRD7 diffractometer, Cu-$K\alpha$ radiation).

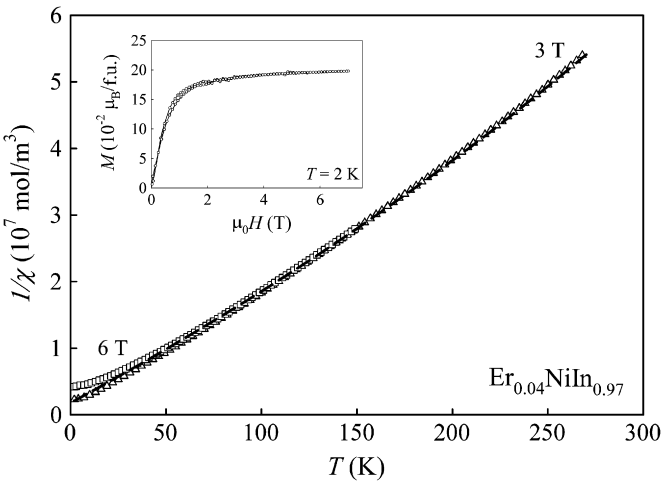

Fig. 9. Temperature dependence of inverse susceptibility in $Er_{0.04}NiIn_{0.97}$, measured in $\mu_o H=3$ T (triangles) and 6 T (squares). The dashed line represents the modified CW fit. Inset: DC magnetization versus magnetic field.

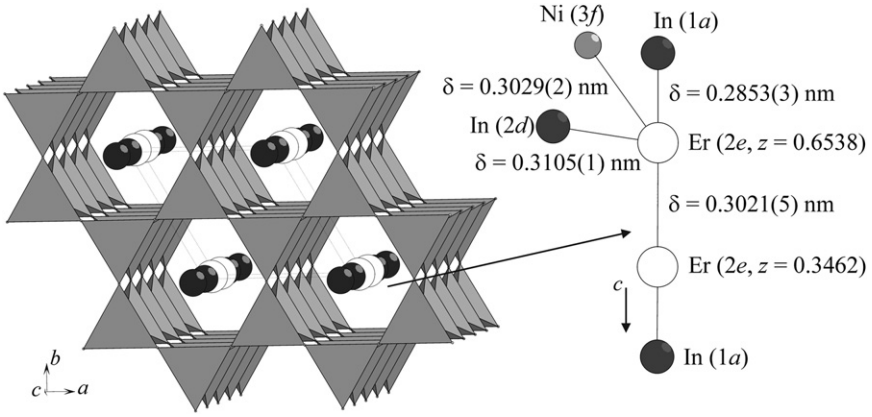

Fig. 8. Close packing of the empty tetrahedra [In(2*d*)3Ni(3*f*)] and sequence of voids occupied by In- and Er-atoms and arrangement of Er atoms along the *c*-direction in $Er_{0.07}NiIn_{0.94}$.

the Er–Ni–In system. The extended homogeneity region of the $ErNi_{1-0.60}In_{1-1.40}$ ternary compounds (ZrNiAl-type structure) with substitution of Ni by In exists in Er–Ni–In system. The $RNi_{1-x}In_{1+x}$ compounds with R=Gd, Tb, Dy, Ho, and Tm also form the homogeneity regions [14,15,22]. In the same time, the compound with this type structure exists in Ce–Ni–In system, but has equiatomic composition. The distinctive feature of Er–Ni–In system is presence of mutual solubilities of $ErNi_2$ ($MgCu_2$-type structure) and $ErNi_4In$ ($MgCu_4Sn$-type structure) phases along 66.7% cross section of Ni. The ternary $ErNi_4In$ can be derived from $ErNi_2$ by substitution of half of Er atoms on In atoms in elementary cell by the scheme: $8ErNi_2=Er_8Ni_{16}=Er_4Er_4Ni_{16}=Er_4In_4Ni_{16}=4ErNi_4In$. The substitution of Er-atoms for In-atoms is possible due to the small difference of atomic radii of these atoms (0.1757 and 0.1663 nm for Er and In, respectively) [23]. A similar situation is observed in the Tm–Ni–In system, in which $TmNi_4In$ forms a continuous series of solid solutions with $TmNi_2$ [24]. Also formation of small homogeneity region of $YbCu_4In$ across the Cu cross section was reported earlier on [25]. As rule, the compounds RCu_4In (R=Y, Nd, Sm, and Gd–Lu) form a continuous series of solid solutions with the RCu_5 compounds ($AuBe_5$ structure type), and in the homogeneity region of these compounds the Cu-atoms are replaced by In atoms [26]. The possibility of substitution of Er-atoms for In-atoms confirms the existence of statistic mixture (Er+In) in the $Er_{2.30}Ni_{1.84}In_{0.70}$ and $Er_{13.53}Ni_{3.14}In_{3.33}$ compounds.

One more interesting fact is the existence of including-substitution type solid solution based on NiIn binary compound. Practically the same situation is observed in R–Pd–In systems (R=Gd–Er), where the large range of solid solutions R_xPdIn_{1-x} (for Er $x=0-0.57$) starting from the binary PdIn (CsCl-type structure) was described [27].

Acknowledgments

The authors would like to express their gratitude to RNDr. Stanislav Daniš, for the X-ray powder data collection. M. Dzevenko is grateful to International Visegrad Fund for support.

References

[1] Ya.M. Kalychak, V.I. Zaremba, R. Pöttgen, M. Lukachuk, R.-D. Hoffmann, Rare earth-transition metal-indides, in: K.A. Gschneider Jr., V.K. Pecharsky, J.-C. Bünzli (Eds.), Handbook on the Physics and Chemistry of Rare Earths, vol. 34, Elsevier, Amsterdam, 2005, pp. 1–133.
[2] Ya.M. Kalychak, Ukr. Chem. J. 64 (7) (1998) 15–20 (in Ukrainian).
[3] Ya.M. Kalychak, Visnyk. Lviv. University, Ser. Khim. 40 (2001) 3–20 (in Ukrainian).
[4] Ya.M. Kalychak, J. Alloys, Compd. 262-263 (1997) 341–345.
[5] M. Dzevenko, Yu. Tyvanchuk, L. Bratash, R. Zaremba, Ya. Galadzhun, V. Zaremba, L. Havela, Ya. Kalychak, 2006, in: Proceedings of the XIIth International Seminar on Physics and Chemistry of Solids, Lviv, Ukraine, May 28–31, 2006, p. 127.
[6] K.H.J. Buschow, J. Less-Common Met. 16 (1968) 45–53.
[7] E. Helner, Z. Metallkd. 41 (1950) 401–406.
[8] Ph. Durussel, G. Burri, P. Feschotte, J. Alloys Compd. 257 (1997) 253–258.
[9] H. Okamoto, J. Phase Equilib. 20 (1999) 540.
[10] S.P. Yatsenko, A.A. Semyanikov, H.O. Shakarov, E.G. Fedorova, J. Less-Common Met. 90 (1983) 95–108.
[11] W. Kraus, G. Nolze, Powder Cell for Windows, Berlin (1999).
[12] G. King, D. Schwarzenbach Latcon, Xtal3.7 System, in: S.R. Hall, D.J. du Boulay, R. Olthof-Hazekamp (Eds.), University of Western, Australia, 2000.
[13] Ya.M. Kalychak, V.I. Zaremba, Yu.B. Tyvanchuk, 1995, in: Proceedings of the VI International Conference on Crystal Chemistry of Intermetallic Compounds, Lviv, Ukraine, September 26–29, 1995, p. 77.
[14] L. Gondek, A. Szytuła, S. Baran, M. Rams, J. Hernandez-Velasco, Yu. Tyvanchuk, J. Magn. Magn. Mater. 278 (2004) 392–396.
[15] Yu.B. Tyvanchuk, Ya.M. Kalychak, L. Gondek, M. Rams, A. Szytuła, Z. Tomkowicz, J. Magn. Magn. Mater. 277 (2004) 368–378.
[16] G.T. Meaden, Electrical Resistance of Metals, Plenum Press, New York, 1965.
[17] M. Dzevenko, D. Mor, Yu. Gorelenko, Ya. Kalychak, 2005, in: Proceedings of the X Scientific Conference Lviv Chemistry Reading, Lviv, Ukraine, May 21–23, 2005, p. H20.
[18] J. Farell, W.E. Wallace, J. Inorg. Chem. 5 (1966) 105–109.
[19] A.K. Larsson, M. Haeberlein, S. Lidin, U. Schwarz, J. Alloys Compd. 240 (1996) 79–84.
[20] J. Rodriguez-Carvajal, Program Fullprof, Laboratoire Leon Brillouin (CEACNRS), 2000.
[21] Yu.B. Tyvanchuk, M. Dzevenko, L. Havela, Ya.M. Kalychak, L.G. Akselrud, H. Ehrenberg, 2007, in: Proceedings of the XIII International Seminar on Physics and Chemistry of Solids, Ustron Slaski, Poland, June 10–13, 2007, p. 84.
[22] M. Lukachuk, Ya.M. Kalychak, R. Pöttgen, Z. Naturforsch. 59b (2004) 893–897.
[23] J. Emsley, The Elements, 2nd ed., Clarendon Press, Oxford, 1991.
[24] M. Lukachuk, Ya.M. Kalychak, T. Nilges, R. Pöttgen, Z. Naturforsch. 60b (2005) 393–397.
[25] I. Felner, I. Nowik, J. Magn. Magn. Mater. 63-64 (1987) 615–617.
[26] Ya.M. Kalychak, Metally 4 (1998) 110–118 (in Russian).
[27] M. Giovannini, A. Saccone, S. Delfino, P. Rogl, Intermetallics 11 (2003) 1237–1243.
[28] Ya.M. Kalychak, L.G. Akselrud, V.I. Zaremba, V.M. Baranyak, Dopov. Akad. Nauk Ukr. RSR, Ser. B 3 (1984) 39–42 (in Ukrainian).
[29] V.I. Zaremba, V.M. Baranyak, Ya.M. Kalychak, Visnyk. Lviv. University, Ser. Khim. 25 (1984) 18–19 (in Ukrainian).
[30] V.I. Zaremba, V.K. Belskii, Ya.M. Kalychak, V.K. Pecharskii, E.I. Gladyshevskii, Dopov. Akad. Nauk Ukr. RSR, Ser. B 3 (1987) 42–43 (in Ukrainian).
[31] M. Dzevenko, Ya. Galadzhun, R. Zaremba, V. Zaremba, R. Pöttgen, Ya. Kalychak, Visnyk. Lviv. University, Ser. Khim. 52 (2011) 67–71 (in Ukrainian).
[32] S. Thimmaiah, J. Weber, G.J. Miller, Z. Anorg. Allg. Chem. 635 (2009) 1831–1839.
[33] R. Ferro, R. Marazza, G. Rambaldi, Z. Metallkd. 65 (1) (1974) 37–39.
[34] V.I. Zaremba, V.A. Bruskov, P.Yu. Zavalij, Ya.M. Kalychak, Neorg. Mater. 24 (1988) 409–411 (in Russian).
[35] Ya.M. Kalychak, V.I. Zaremba, V.M. Baranyak, P.Yu. Zavalij, V.A. Bruskov, L.V. Sysa, O.V. Dmytrakh, Neorg. Mater. 26 (1990) 94–96 (in Russian).
[36] U.Ch. Rodewald, M. Lukachuk, B. Heying, R. Pöttgen, Monatsh. Chem. 137 (2006) 7–13.
[37] V.I. Zaremba, Ya.M. Kalychak, P.Yu. Zavalij, V.A. Bruskov, Kristallografiya 36 (1991) 1415–1418 (in Russian).
[38] M. Lukachuk, Ya.M. Kalychak, M. Dzevenko, R. Pöttgen, J. Solid State Chem. 178 (4) (2005) 1247–1253.
[39] M. Lukachuk, Ya.V. Galadzhun, R.I. Zaremba, M.V. Dzevenko, Ya.M. Kalychak, V.I. Zaremba, U.Ch. Rodewald, R. Pöttgen, J. Solid State Chem. 178 (9) (2005) 2724–2733.